SACLANTCEN Report SR- 49

SACLANTCEN Report
SR – 49

SACLANT ASW RESEARCH CENTRE REPORT

DETERMINISTIC PROPAGATION MODELLING

by

WILLIAM A. KUPERMAN and FINN B. JENSEN

PART I: FUNDAMENTAL PRINCIPLES

PART II: NUMERICAL RESULTS

1 JUNE 1981

NORTH ATLANTIC TREATY ORGANIZATION

LA SPEZIA, ITALY

SACLANTCEN REPORT SR-49

NORTH ATLANTIC TREATY ORGANIZATION

SACLANT ASW Research Centre
Viale San Bartolomeo 400 - I-19026 San Bartolomeo (SP), Italy.

tel: national 0187 560940
international + 39 187 560940

DETERMINISTIC PROPAGATION MODELLING

by

William A. Kuperman and Finn B. Jensen

Part I: Fundamental Principles

Part II: Numerical Results

(Reprinted from BJØRNØ, L. ed. Underwater Acoustics and Signal Processing. Dordrecht, Netherlands, Reidal Pub Coy, 1981: pp 125-141)

1 June 1981

This report has been prepared as part of Project 19.

APPROVED FOR DISTRIBUTION

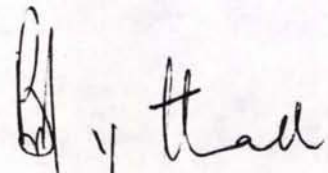

B.W. LYTHALL
Director

DETERMINISTIC PROPAGATION MODELLING I: FUNDAMENTAL PRINCIPLES

W.A. Kuperman and F.B. Jensen

NATO SACLANT ASW Research Centre, La Spezia, Italy

ABSTRACT The physics of sound propagation in the ocean is briefly reviewed. The wave equation is presented and a set of solutions under a variety of approximations are discussed. The consistency among these solutions is illustrated.

INTRODUCTION

This and the next papers [1,2] form a brief introduction to ocean acoustic modelling. Here we present a basic set of deterministic acoustic models. In the following paper we use computer versions of these acoustic models to provide a deeper insight into the physical processes that govern sound propagation in the ocean. The third paper discusses the additional complication of the ocean being a stochastic medium.

I. SOUND PROPAGATION IN THE OCEAN

The goal of ocean acoustic modelling is to describe sound propagation phenomena in the ocean quantitatively. To clarify the complexity of the modelling problem, let us briefly review the environmental acoustics of the ocean. Figure 1 is a schematic of some propagation paths in the ocean; we show two possible locations of sources of sound on the left and sound is propagating to the right. The two dashed lines are sound-speed profiles that vary with both depth and range. Lines A, B, C, and D represent four possible propagation paths. The shapes of the paths are determined by the location of the source and the sound-speed structure over the extent of the propagation.

L. Bjørnø (ed.), Underwater Acoustics and Signal Processing, 125–132.

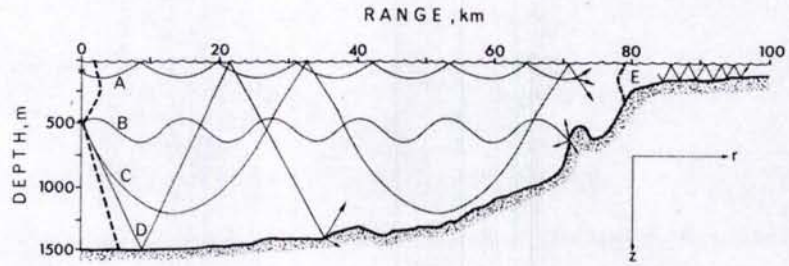

Fig. 1 Representation of sound propagation in the ocean

Path A from the shallow source is "surface-duct" propagation, because the sound-speed profile is such that the sound is trapped near the surface of the ocean. Paths B, C, and D are from the deeper source. Ray B, leaving the source at a small angle from the horizontal, will tend to propagate in the "deep sound channel" without interacting with the boundaries (surface and bottom) of the ocean. At slightly steeper angles (path C) we have "convergence zone" propagation, which is a spatially periodic phenomenon of zones of high intensity near the surface. Here the path interacts with the ocean surface but not with the bottom. Path D is the "bottom-bounce path", which has a shorter cycle period than the convergence zone path. The right-hand side of Fig. 1 depicts propagation on the continental shelf (shallow waters) where a complicated bottom structure combined with variable sound-speed profiles result in rather complicated propagation conditions not always suited for a simplistic ray picture representation.

A consistent mathematical model must contain the physics that govern all of these paths of propagation. Here we will state the mathematical model generally accepted to describe deterministic sound propagation in the ocean. We will then present various solutions and approximations that are themselves often referred to as acoustic models. Greater detail will be found in [3 to 11].

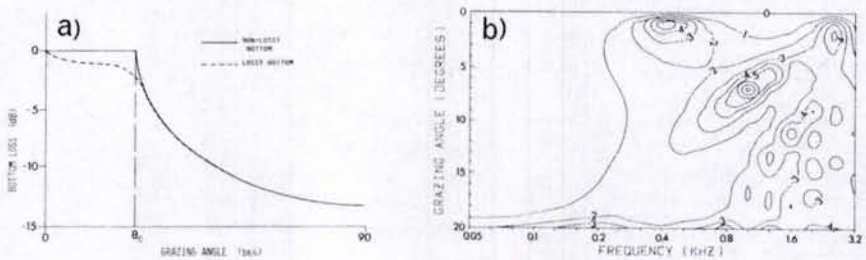

Fig. 2 Bottom reflection loss vs grazing angle and frequency

II. LOSS MECHANISMS

Our ability to effectively model acoustic propagation in the ocean is aided by studying the loss mechanisms associated with ocean sound propagation: aside from geometric spreading there is volume attenuation loss, bottom loss, and surface and bottom scattering loss.

Volume attenuation increases with increasing frequency. Returning to Fig. 1, the loss most associated with path B will in general be volume attenuation, because this path does not involve interaction with the boundaries. Since there is very little attenuation at low frequencies, deep-sound-channel propagation has been observed to distances of many thousands of kilometres.

When sound interacts with the bottom, the nature of the bottom becomes important. Figure 2a depicts simple bottom loss curves with zero dB loss indicating perfect reflection. For a "non-lossy" bottom we still get severe loss above a certain critical angle θ_c, which results in loss in the water column due to transmission into the bottom. However, for the "lossy" (more realistic) bottom we never get perfect reflection, even though the curves look similar. Path D in Fig. 1, the bottom-bounce path, often corresponds to angles near or above the critical angle; therefore after a few bounces, it will be highly attenuated. On the other hand, for shallower angles, many more bounces are possible; hence in shallow water (path E) most of the energy that propagates is close to the horizontal. In reality, much of the ocean bottom is layered and bottom loss then becomes a complicated function of frequency and grazing angle. Figure 2b displays some model results of loss contours of a layered bottom; the more familiar loss vs grazing angle curves for a single frequency is obtained from a vertical cut through the loss contours. For example, at low frequencies Fig. 2b indicates a critical angle of about 18° whereas at high frequencies we do not see a critical angle.

Surface and bottom scattering loss is discussed in [2].

III. THE MATHEMATICAL MODEL

The mathematical model we use for sound propagation in the ocean is the wave equation (with its associated boundary conditions) for a harmonic point source with time dependence $\exp(-i\omega t)$

$$\nabla^2\phi(x,y,z)+\left[\frac{\omega}{c(x,y,z)}\right]^2\phi(x,y,z) = -\delta(x-x_o)\delta(y-y_o)\delta(z-z_o) \quad (1)$$

At any point (x,y,z) in the medium the velocity potential ϕ satisfies Eq. 1 where c(x,y,z) is the sound speed of the medium and δ is the Dirac delta function; hence the right-hand side of Eq. 1 describes a point source at the position (x_o, y_o, z_o). Boundary conditions can be derived by requiring continuity of such physical quantities as particle velocity and pressure [4]:

$$v_i = -\frac{\partial \phi}{\partial x_i} \; ; \quad x_i = x, y, \text{ or } z. \tag{2}$$

$$p = -i\omega\rho\phi \tag{3}$$

For the boundary conditions we begin with the ocean surface. The density of air is negligible compared with that of water; hence the pressure must vanish ("pressure-release surface") at the ocean surface. Thus, from Eq. 3, ϕ vanishes at the ocean surface. At a boundary between two media such as the ocean and the ocean bottom, the balancing of forces at the interface requires that both the normal particle velocity and the sound pressure be continuous across the boundary; hence, the right-hand sides of both Eqs. 2 and 3 must be continuous across the boundary. Of course these boundary conditions are more complicated for elastic media, which also support shear waves.

IV. ACOUSTIC MODELS

Here we discuss the four acoustic models displayed in Fig. 3.

Ray theory is a high-frequency approximation to solving Eq. 1. A solution of the form

$$\phi = G(x,y,z)\, e^{iS(x,y,z)} \tag{4}$$

is inserted into Eq. 1 and we assume that G does not change much within an acoustic wavelength (high-frequency approximation or

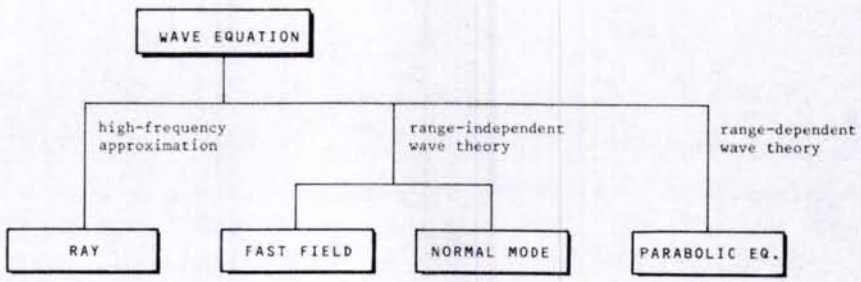

Fig. 3 Four acoustic models

geometrical-acoustics approximation). We must eventually solve the Eikonal equation [4], which leads to the ray equations. We give an example of a solution below and in the next paper [1].

Range-Independent Wave Theory solves the wave equation exactly when the ocean environment does not change in range (in the cylindrical coordinate r as indicated in Fig. 1). One of many possible derivations of this solution technique is to Fourier decompose the acoustic field into an infinite set of horizontal waves:

$$\phi = \frac{1}{(2\pi)^2} \int d^2\vec{\eta}\; u(\vec{\eta},z)\; e^{i\vec{\eta}\cdot\vec{r}} \tag{5}$$

where, from Eq. 1, we find that $u(\eta,z)$ satisfies the equation

$$\frac{d^2u}{dz^2} + \left[k^2(z) - \eta^2\right]u = -\delta(z-z_o)\;;\; k = \frac{\omega}{c}\;. \tag{6}$$

It turns out [12] that after further manipulation, Eq. 5 can be effectively evaluated using an FFT; however, because of the parameter η, Eq. 6 must be numerically solved for many values of η. This direct numerical solution is the Fast Field Program method (FFP).

Rather than directly solve Eq. 6 we can make a "normal-mode expansion" solution of Eq. 6; let $u = \Sigma\, a_n u_n(z)$, where the u_n's are the solution of the eigenvalue (k_n) equation:

$$\frac{d^2u_n}{dz^2} + \left[k^2(z) - k_n^2\right] u_n = 0 \tag{7}$$

satisfying the boundary conditions discussed in Section III. After some considerable manipulation and integration (of Eq. 5), the solution to the wave equation becomes [13]:

$$\phi = \frac{i\rho(z_o)}{(8\pi r)^{\frac{1}{2}}}\, e^{-i\pi/4} \sum \frac{u_n(z_o)u_n(z)}{k_n^{\frac{1}{2}}}\; e^{i(k_n r-\omega t)} \tag{8}$$

The loss mechanisms appear in Eq. 8 because the eigenvalues, k_n turn out to have positive imaginary parts [13], thereby resulting in an exponential attenuation in each normal-mode term of the acoustic field. Equation 8 is a "far-field" solution of the wave equation and neglects the "continuous spectrum" of modes; therefore we consider only a discrete number of modes. In effect, if we look at a ray picture of the modes we can associate a grazing angle at the ocean bottom with each of the modes: the continuous part of the mode spectrum corresponds to rays with grazing angles greater than the critical angle and this sound suffers severe loss.

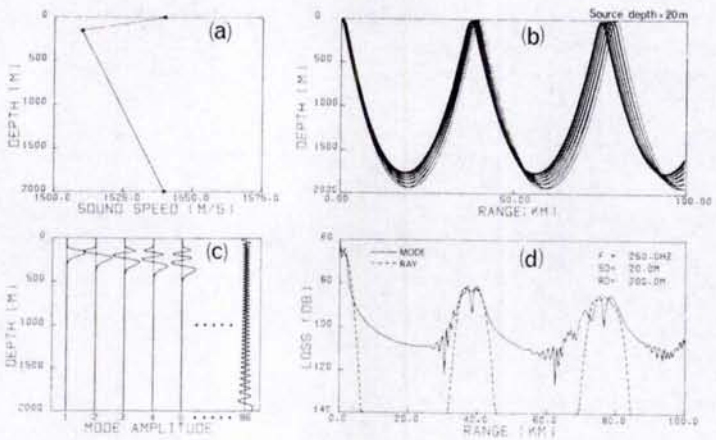

Fig. 4 Deep-water convergence-zone propagation

Since the range-independent wave-theory solution is more or less an exact solution of the wave equation and ray theory is a high-frequency solution, there should be overlapping regimes where both solutions are approximately the same. Figure 4 displays such an example of deep-water convergence-zone propagation. The upper part gives (a) the sound-speed profile and (b) a ray-trace result showing periodic focusing of the rays near the surface. The lower part displays (c) the shape of the 86 modes numerically calculated from Eq. 7 and (d) the propagation loss as calculated both by ray-theory methods (using the density of rays) and mode methods (performing the summation of Eq. 8). In the mode picture, the zones of high intensities arise from the interference pattern resulting from the coherent addition of the modes.

The Parabolic Equation Method [14] is a far-field narrow-angle approximation to the wave equation. It is most accurate when propagation with respect to the horizontal is confined within a cone of about ± 20°. Essentially we make the approximation that

$$\phi = G(r,z)\ S(r). \tag{9}$$

S will satisfy an average propagation equation and will be a rapidly varying function in range. The parabolic approximation is to assume that because the environment is changing slowly with range, $(\partial^2 G/\partial r^2) << 2k_o (\partial G/\partial r)$, where k_o is an average wavenumber. This leads to an equation for G^o with only the first derivative of G with respect to r. This approximation takes us from a boundary-value wave-equation problem to an initial-value parabolic equation that lends itself to marching-solution techniques. Numerical results will be given in the next paper [1].

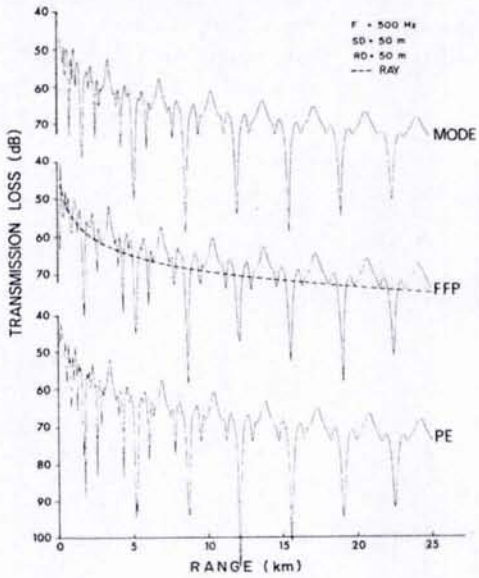

Fig. 5 Inter-model comparison for shallow-water environment

H_w = 100 m
c_w = 1500 m/s
c_b = 1550 m/s
ρ_b = 1.2 g/cm^3
β_b = 1.0 dB/λ

Since we are essentially attempting to solve the same equation (the wave equation), we should find situations where all four models give the same results. Figure 5 is a shallow-water example where we see that the wave-theory models give virtually identical results. The ray model, though it cannot reproduce the interference pattern, does yield the same approximate level.

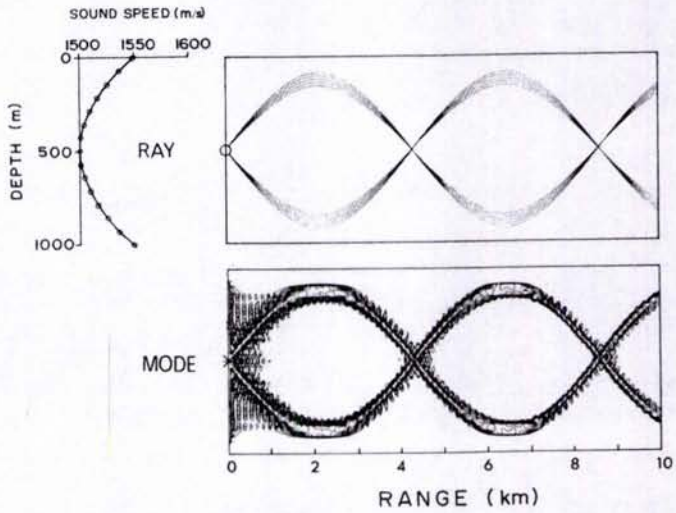

Fig. 6 Correspondence between ray and normal-mode solutions

We mentioned earlier that there is some ray-mode correspondence and we further illustrate this in Fig. 6, which shows a ray trace of some up and downgoing rays in a deep sound-channel type environment. Figure 6 also shows contoured loss from a normal-mode model where we have limited the modes to correspond to the appropriate ray angles. This same pattern, which appears in both pictures, demonstrates the underlying consistency between these models. The near-field differences are well-understood wave-diffraction effects.

SUMMARY

We have briefly presented a set of acoustic models and at the same time tried to explain their underlying physical principles. We have also illustrated the consistency between the models. In the next paper [1] we shall apply computer versions of these models to extract further information about the nature of sound propagation in the ocean.

REFERENCES

1. JENSEN, F.B. and KUPERMAN, W.A. (This volume).
2. SCHNEIDER, H.G. (This volume).
3. BREKHOVSKIKH, L.M. Waves in Layered Media. Academic, 1960.
4. OFFICER, C.B. Introduction to the Theory of Sound Transmission. McGraw Hill, 1958.
5. TOLSTOY, I. and CLAY, C.S. Ocean Acoustics: Theory and Experiment in Underwater Sound. McGraw Hill, 1966.
6. TOLSTOY, I. Wave Propagation. McGraw Hill, 1973.
7. CLAY, C.S. and MEDWIN, H. Acoustical Oceanography. Wiley, 1977.
8. URICK, R.J. Principles of Underwater Sound. McGraw Hill, 1975.
9. KELLER, J.B. and PAPADAKIS, J.S. Wave Propagation and Underwater Acoustics. Springer-Verlag, 1977.
10. DE SANTO, J.A. Ocean Acoustics. Springer-Verlag, 1979.
11. WILLIAMS, A.O. In: STEPHENS, R.W.B. ed. Underwater Acoustics. Wiley-Interscience, 1970.
12. DINAPOLI, F.R. and DEAVENPORT, R.L. J.Acoust.Soc.Am., 67, 1980: 92-105.
13. INGENITO, F., FERRIS, H., KUPERMAN, W.A. and WOLF, S.N. Shallow-water acoustics, NRL Rpt 8179, U.S. Nav. Res. Lab., 1978.
14. TAPPERT, F. In: [9].

DETERMINISTIC PROPAGATION MODELLING II: NUMERICAL RESULTS

F.B. Jensen and W.A. Kuperman

NATO SACLANT ASW Research Centre, La Spezia, Italy

ABSTRACT The most commonly used propagation models are presented and their areas of applicability are indicated. Furthermore, the use of these models for gaining insight into the physical mechanisms governing sound propagation in the ocean is illustrated through a sequence of modelling examples.

INTRODUCTION

This is the second of three papers dealing with sound-propagation modelling in the ocean [1,2]. Here we present some numerical results that include comparison with broadband experimental data from various ocean environments, simulation studies of propagation over sloping bottoms, and a study of seismic propagation in terms of bottom-interface waves.

I. MODEL APPLICABILITY

To indicate with some precision the type of ocean environment for which a given model should be used, we have classified environments according to water depth, frequency, and environmental complexity, as shown in Table 1 [3]. Here shallow water indicates all water depths for which sound interacts significantly with the ocean bottom. The separation frequency of 500 Hz between the low- and high-frequency regimes is arbitrarily chosen.

When indicating the applicability of a propagation model to a given type of environment we take into consideration limitations

L. Bjørnø (ed.), Underwater Acoustics and Signal Processing, 133–142.

Table 1 Applicability of propagation models

MODEL TYPE	APPLICATIONS							
	SHALLOW WATER				DEEP WATER			
	LF		HF		LF		HF	
	RI	RD	RI	RD	RI	RD	RI	RD
RAY			◪	◪	◪	◪	◪	◪
NORMAL MODE	■		■		■		◪	
FAST FIELD (FFP)	■		■		■		■	
PARABOLIC EQ.(PE)	◪	◪			◪	◪	◪	◪

LF: LOW FREQUENCY (< 500 Hz) RI: RANGE-INDEPENDENT ENVIRONMENT
HF: HIGH FREQUENCY (> 500 Hz) RD: RANGE-DEPENDENT ENVIRONMENT

in the underlying theory. Thus ray models are applicable only to high-frequency propagation, and only some models (ray, PE) can handle a range-dependent environment. When indicating a model's practicality we consider exclusively the running time. Thus the time increases with both frequency and water depth for some models (mode, PE), while the time is relatively independent of these parameters for the other models. Likewise, running time is proportional to the number of profiles in a range-dependent environment for a ray model, while a PE model takes essentially the same time for range-dependent and range-independent environments.

Full box shading in Table 1 means that a model is applicable as well as practical. On the other hand, if a box is only partially shaded, it means that the model is applicable with caution (theoretical limitations), or that running times are excessive. The above judgements are, of course, relative. That is, for columns that did not originally have a fully-shaded box, we selected the model we felt was the most practical and denoted it by a fully shaded box. For a column where more than one box is fully shaded, the choice of model will depend on the actual models on hand, the running time, input/output options available, etc.

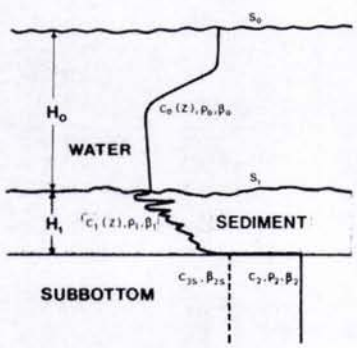

Fig. 1 Environmental input to acoustic models

c_i : compressional speed
c_{2s} : shear speed
ρ_i : density
β_i : compressional att.
β_{2s} : shear attenuation
s_i : rms roughness

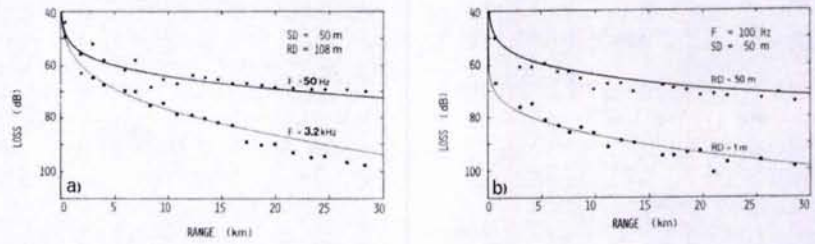

Fig. 2 Model predictions (lines) and experimental data (dots) for shallow-water area in Mediterranean

II. MODEL/DATA COMPARISON

To demonstrate the accuracy to which propagation in a complicated ocean environment can be described by a numerical model, we present comparisons between model results and some broadband experimental data averaged in 1/3 octave bands. Figure 1 shows the type of environmental description used as input to the numerical model.

The first data set presented (Fig. 2) was collected in 110 m of almost isothermal water in the Mediterranean. The theoretical curves given in Fig. 2 were obtained from a normal-mode model. We see that there is excellent agreement between theory and experiment for two widely different frequencies (Fig. 2a) and for two different receiver depths (Fig. 2b).

The second example (Fig. 3) presents data collected in a range-independent shallow-water area in the Atlantic. The environmental input to a normal-mode model is given in Fig. 3a, while

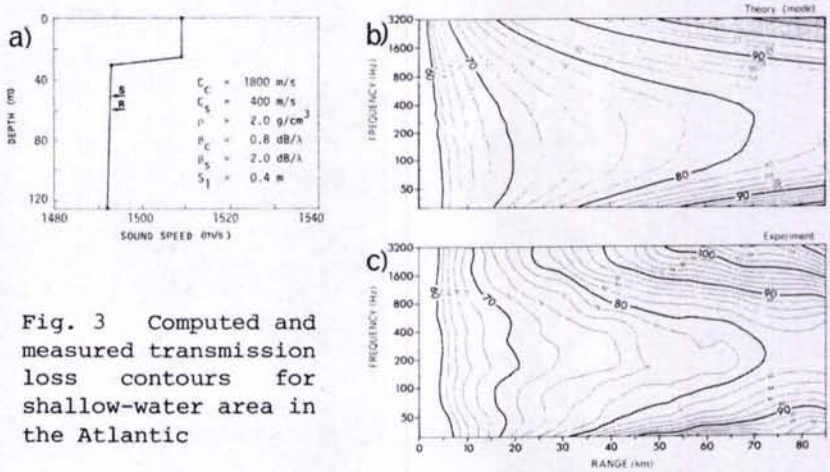

Fig. 3 Computed and measured transmission loss contours for shallow-water area in the Atlantic

the computed loss versus frequency and range is shown in Fig. 3b in the form of an iso-loss contour plot. The experimental data are displayed in Fig. 3c. We notice an extraordinary agreement between theory and experiment. Thus the maximum deviation is only a few decibels for data covering as much as seven octaves of frequencies and a range of more than 80 km. This result was obtained after including shear waves in the bottom and a pronounced sea-floor roughness.

The contour plots in Fig. 3 demonstrate the existence of an optimum propagation frequency around 250 Hz. The optimum frequency is a general phenomenon associated with ducted propagation, and it occurs as a result of competing propagation and attenuation mechanisms at high and low frequencies. In the high-frequency regime volume and scattering loss simply increase with frequency. At lower frequencies the situation is more complicated. With increasing wavelength the efficiency of the duct to confine sound decreases. Hence propagation and attenua-

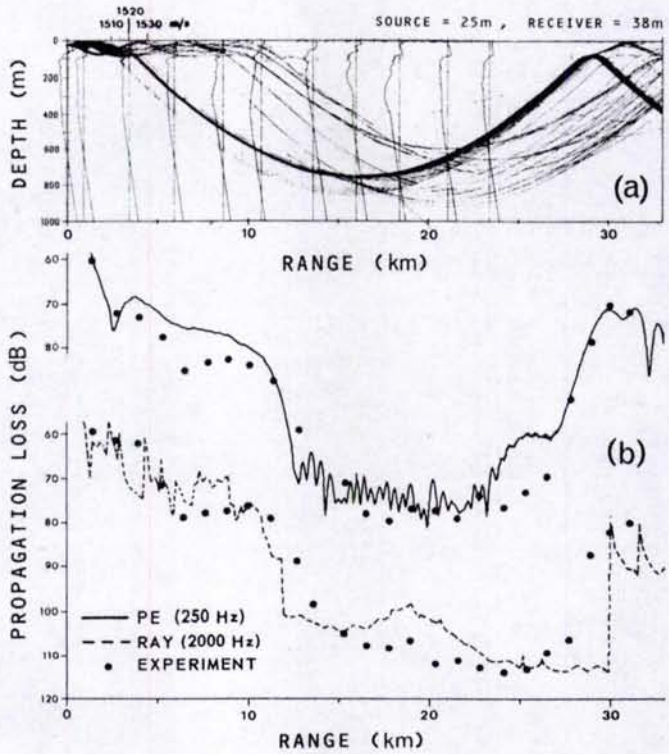

Fig. 4 Model/data comparison of transmission loss for deep-water area in the Mediterranean

tion mechanisms outside the duct (e.g. in the sea floor) affect the intensity of sound in the duct. In fact, the increased penetration of sound into the ocean bottom with decreasing frequency causes the overall attenuation of sound in the water column to increase with decreasing frequency. Thus we get high attenuation at both high and low frequencies, while intermediate frequencies have the lowest attenuation. In typical shallow-water areas the optimum frequency is found to be a few hundred hertz, but it depends strongly on the environment.

In the next example (Fig. 4) we present some deep-water data for a range-varying environment. A ray-trace result superimposed on measured sound-speed profiles is shown in Fig. 4a. We see how sound is trapped in the surface duct out to a range of about 10 km. At this point the surface duct disappears, and almost all energy leaks down in the main body of the water column. Propagation-loss data for two different frequencies are compared with both a PE and a ray solution. We see that the model results are in excellent agreement with the data.

III. PROPAGATION OVER A SLOPING BOTTOM

In this section we demonstrate the range-dependent capability of the PE model by studying sound propagation over a sloping bottom [4,5]. First we consider up-slope propagation for the environment given in Fig. 5. The slope is 0.85° and the frequency is 25 Hz. The water is taken to be isovelocity with a speed of 1500 m/s, while the bottom is characterized by a speed of 1600 m/s, a density of 1.5 g/cm^3, and an attenuation of 0.2 dB/wavelength.

Before interpreting the contour plot, let us have a look at the simplified sketch in the upper part of Fig. 5. Using the ray/mode analogy, a given mode can be associated with up- and down-going rays with a specific grazing angle. The sketch indicates a ray corresponding to a given mode. As sound propagates up the slope, the grazing angle for that particular ray (mode) increases, and at a certain point in range the angle exceeds the critical angle at the bottom, meaning that the reflection loss becomes very large and that the ray essentially leaves the water column and starts propagating in the bottom. The point in range where this happens corresponds to the cut-off depth for the equivalent mode.

To emphasize the main features in Fig. 5, we have chosen to display contour levels between 70 and 100 dB in 2 dB intervals. Thus high-intensity regions (loss < 70 dB) are given as blank areas within the wedge, while low-intensity regions (loss > 100 dB) are given as blank areas in the bottom. In this parti-

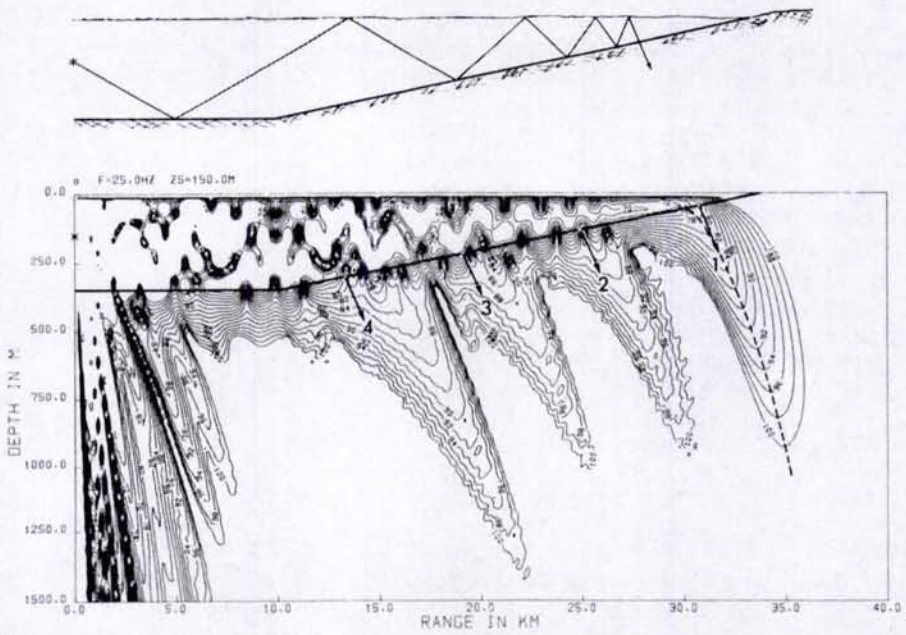

Fig. 5 Predicted characteristics of the acoustic field for up-slope propagation

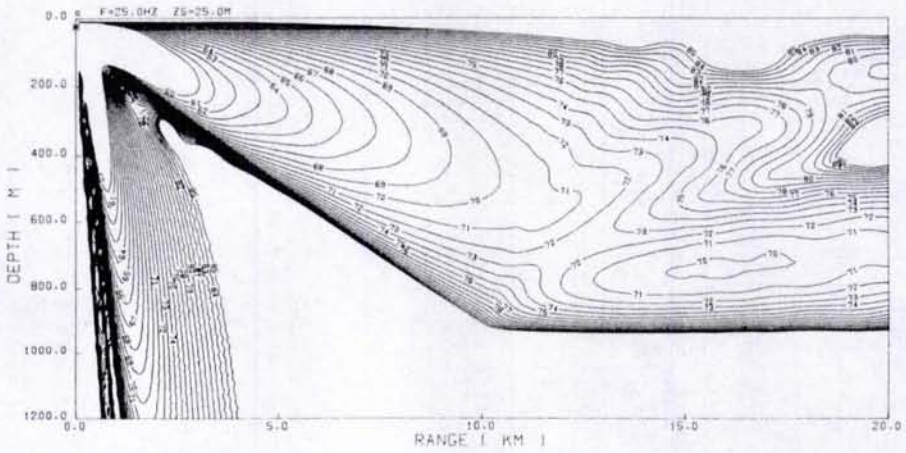

Fig. 6 Predicted characteristics of the acoustic field for down-slope propagation

cular case four modes are excited at the source. As sound propagates up the slope we see four well-defined beams in the bottom, one corresponding to each of the four modes. This phenomenon of energy leaking out of the propagation channel as discrete beams has been confirmed experimentally [6].

We now consider the problem of down-slope propagation as illustrated in Fig. 6. Water and bottom properties are as in the former example. The initial water depth is 50 m, and the bottom slope is 5° out to a range of 10 km. Beyond 10 km the bottom is flat. Only one mode is excited at the source, while as many as 11 modes can exist in the deep part beyond a range of 10 km. The regularity of the contour lines out to 10 km indicates that only one mode is excited while propagating down the slope. Beyond 10 km the contour lines become more complicated, indicating that the abrupt change in slope at 10 km causes a redistribution of energy among existing modes. Thus mode coupling seems to be associated with abrupt changes in bottom slope rather than with the slope itself.

IV. SEISMIC PROPAGATION

This last section demonstrates the capability of the FFP model in handling propagation in a multilayered environment where shear properties are included in all layers. If the bottom can support shear waves there will exist a surface wave that travels along the water/bottom interface. Indeed, a surface wave will

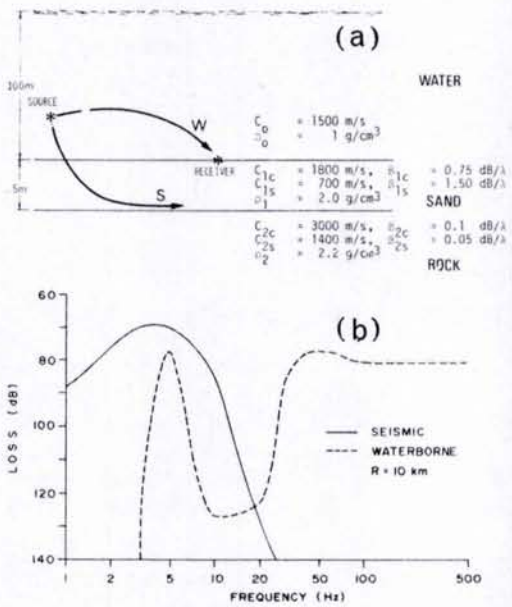

Fig. 7 Predicted loss versus frequency for seismic and waterborne paths

exist at the interface between any two media if at least one of them can support shear waves. An important feature of these surface waves is that they have no frequency cut-off, whereas, for a particular water depth, waterborne propagation cuts off below a frequency that is a function of the environmental conditions.

We are going to investigate this phenomenon theoretically using the FFP model. Figure 7a displays a typical shallow-water environment: there is a 5 m sediment layer of fairly compact sand overlying a sedimentary rock basement. Hence, from the discussion above, two surface waves should exist: one at the water/sand interface and the other at the sand/rock interface. However, due to the high shear attenuation in the sand (1.5 dB/wavelength) it turns out that only the wave at the sand/rock interface gives appreciable contribution to the acoustic field at the water/bottom interface.

In Fig. 7b is shown the computed loss versus frequency at a range of 10 km for both the seismic and the waterborne paths. We see that the waterborne sound propagates well above 50 Hz, while seismic sound propagates well below 10 Hz. In the intermediate frequency range around 20 Hz the propagation is poor. Thus, for a receiver located on the ocean bottom, seismic propagation paths are important only at very low frequencies. Also this phenomenon has been verified experimentally [7].

SUMMARY

We have briefly presented an overview over the most commonly used propagation models, pointed out their areas of applicability, and demonstrated the particular features of the various models through a series of examples that included comparison with experimental data and simulation studies of particular propagation phenomena.

REFERENCES

1. KUPERMAN, W.A. and JENSEN, F.B. (This volume).
2. SCHNEIDER, H.G. (This volume).
3. JENSEN, F.B. and KUPERMAN, W.A. SACLANTCEN SR-34, La Spezia, Italy, SACLANT ASW Research Centre, 1979.
4. JENSEN, F.B. and KUPERMAN, W.A. J.Acoust.Soc.Am., 67, 5, 1980.
5. JENSEN, F.B. and KUPERMAN, W.A. In: KUPERMAN, W.A. and JENSEN, F.B. eds. Bottom-Interacting Ocean Acoustics. New York, Plenum Press, 1980.
6. COPPENS, A.B. and SANDERS, J.V. In: as [5].
7. RAUCH, D. In: as [5].

DISCUSSION

Comment: L. BJØRNØ.

In the figure showing the up-slope propagation you did not include shear waves in the propagation calculation. Which influence would you anticipate from shear waves on the patterns of intersity distributions ?

Reply: F. JENSEN.

Our study of sound propagation in a wedgeshaped ocean was done with the PE model, which cannot handle shear waves in the bottom. I do not know of any numerical model that can solve the problem for a solid bottom, but it is definitely an interesting question.

Comment: W.J. VETTER.

Can you comment on the subbottom depths which have practically important effects on the propagation (in range) ?

Reply: F. JENSEN.

We have studied this problem in some detail (F.B. Jensen "The effect of the ocean bottom on sound propagation in shallow water". In "Sound propagation and Underwater Systems", R.H. Clarke (ed.). Imperial College, London, 1978), and it is generally sufficient to know bottom properties to a depth of one to two acoustic wavelengths.

Comment: P. SCHULTHEISS.

How sensitive is the model to precise knowledge of bottom parameters ?

Reply: F. JENSEN.

In cases where sound interacts strongly with the ocean bottom (shallow water) the model output is very sensitive to bottom parameters such as sound velocity and attenuation. Even an "intelligent" guess of these parameters can lead to prediction errors of 10-20 dB at longer ranges.

Comment: A. WASILJEFF.

Is it possible to include rough boundaries in some of your models ?

Reply: F. JENSEN.

Rough-boundary scattering loss is included in most of the models. However, this particular feature of the models has not yet been well tested due to a lack of experimental data.

INITIAL DISTRIBUTION

	Copies
MINISTRIES OF DEFENCE	
MOD Belgium	2
DND Canada	10
CHOD Denmark	8
MOD France	8
MOD Germany	15
MOD Greece	11
MOD Italy	10
MOD Netherlands	12
CHOD Norway	10
MOD Portugal	5
MOD Turkey	5
MOD U.K.	16
SECDEF U.S.	61
NATO AUTHORITIES	
Defence Planning Committee	3
NAMILCOM	2
SACLANT	10
SACLANTREPEUR	1
CINCWESTLANT/COMOCEANLANT	1
COMIBERLANT	1
CINCEASTLANT	1
COMSUBACLANT	1
COMMAIREASTLANT	1
SACEUR	2
CINCNORTH	1
CINCSOUTH	1
COMNAVSOUTH	1
COMSTRIKFORSOUTH	1
COMEDCENT	1
COMMARAIRMED	1
CINCHAN	1

	Copies
SCNR FOR SACLANTCEN	
SCNR Belgium	1
SCNR Canada	1
SCNR Denmark	1
SCNR Germany	1
SCNR Greece	1
SCNR Italy	1
SCNR Netherlands	1
SCNR Norway	1
SCNR Portugal	1
SCNR Turkey	1
SCNR U.K.	1
SCNR U.S.	2
SECGEN Rep. SCNR	1
NAMILCOM Rep. SCNR	1
NATIONAL LIAISON OFFICERS	
NLO Canada	1
NLO Denmark	1
NLO Germany	1
NLO Italy	1
NLO U.K.	1
NLO U.S.	1
NLR TO SACLANT	
NLR Belgium	1
NLR Canada	1
NLR Denmark	1
NLR Germany	1
NLR Greece	1
NLR Italy	1
NLR Netherlands	1
NLR Norway	1
NLR Portugal	1
NLR Turkey	1
NLR UK	1
NLR US	1
Total initial distribution	236
SACLANTCEN Library	10
Stock	34
Total number of copies	280